

GRAPH-BASED REPRESENTATION FOR 2-D SHAPE USING DECOMPOSITION SCHEME

Duck Hoon Kim[†], Il Dong Yun[‡], and Sang Uk Lee[†]

[†]School of EECS, Seoul National University, Seoul, 151-742, Korea

[‡]School of EIE, Hankuk University of Foreign Studies, Yongin, 449-791, Korea
ducks@diehard.snu.ac.kr, yun@hufs.ac.kr, and sanguk@ipl.snu.ac.kr

ABSTRACT

In this paper, to represent 2-D shape as a relational structure, *i.e.* graph, we propose a new shape decomposition scheme composed of two stages: First, a given shape is decomposed into meaningful parts by using the constrained morphological decomposition (CMD) in a recursive manner. More specifically, the CMD adopts the use of the *opening* operation with the ball-shaped structuring element and the *weighted convexity* to select the optimal decomposition. Second, the iterative merging stage provides a compact graph-based representation based on the weighted convexity difference. From the experimental results for various and modified 2-D shapes, it is believed that the graph-based representation for 2-D shape coincides with that based on human insight, and also provides robustness to scaling, rotation, noise, shape deformation and occlusion.

1. INTRODUCTION

Recently, it is of an important issue to develop part-based representations for 2-D shape, which decomposes a given shape into canonically meaningful parts, since this allows a relational structure, *i.e.* graph, to be generated directly for further shape-related applications such as those involving content-based retrieval, object recognition, and so on. So far, various part-based representations, which can be converted into graphs, have been developed, and they are categorized into morphology-based [1] and partition-based [2, 3] decomposition. The morphology-based decomposition includes a well-developed mathematical structure, based on simple and intuitive interpretations using geometric terms of the shape, size and location [1]. However, it is sensitive to scaling, rotation and noise since most structuring elements (SE's) cannot approximate well their target shapes in a continuous domain. The partition-based decomposition implies that a given shape is divided into proper connected components by connecting points on the shape's boundary, thus this system provides a simple and efficient means of creating an intuitive description. Moreover, it is invariant to scaling and rotation as well as being robust to noise. However, it involves heavy computational complexity due to the

need to compute each part in reaction-diffusion space [2], or requires a means of specifying the number of parts to be decomposed [3].

In this paper, a new shape decomposition scheme for 2-D shape is proposed in order to provide a graph-based representation. The proposed scheme stands on two psychological rationales: One is that a human being recognizes an object by its part structure [4], and the other is that the parts are generally defined as being either convex or nearly convex shapes [2, 3]. To convert these rationales into a practical application, the proposed scheme combines the advantages of the morphology-based decomposition such as simple and intuitive operations with those of the partition-based decomposition such as the perceptually valid measure, *convexity* [3]. Actually, the proposed scheme recursively performs the constrained morphological decomposition (CMD) based on the *opening* operation with the ball-shaped SE's and the *weighted convexity*. Note that the parts to be decomposed are rendered convex or nearly convex by using the ball-shaped SE since it is convex itself and rotation-invariant. Then a *merging criterion* employing the weighted convexity difference, which determines whether adjacent parts are to be merged or not, is adopted in order to provide a compact representation. These procedures are summarized as two stages, *i.e.*, the recursive decomposition stage (RDS) and the iterative merging stage (IMS).

This paper is organized as follows: In Section 2, we describe the CMD first, and then the shape decomposition scheme composed of RDS and IMS in Section 3. Section 4 presents experimental results for various and modified 2-D shapes. Finally, Section 5 concludes this paper.

2. CONSTRAINED MORPHOLOGICAL DECOMPOSITION

In this section, we present the notion of CMD composed of two steps: The first step consists of generating candidates for the next step using the *opening* operation as the size of the ball-shaped SE varies. The second step is to select the best candidate in the form of the output of the CMD using the *weighted convexity*.

2.1. Generating parts using the opening operation

The ball-shaped SE, $\mathbf{S}(k)$, is

$$\mathbf{S}(k) = \begin{cases} 1, & \text{if } \|\mathbf{u} - \mathbf{o}\|_2 \leq k, \\ 0, & \text{if } \|\mathbf{u} - \mathbf{o}\|_2 > k, \end{cases} \quad (1)$$

where \mathbf{u} and \mathbf{o} refer to a point and the central point of the binary image, in which “1” represents the boundary and interior while “0” represents the exterior, respectively, and $\|\cdot\|_2$ refers to the Euclidean distance. Note that the natural number, k , represents the radius of the ball-shaped SE.

Let us assume that \mathbf{M} is a binary image which describes a 2-D shape, and $\mathbf{M} \circ \mathbf{S}(k)$ and $\mathbf{M} - \mathbf{M} \circ \mathbf{S}(k)$ are derived from the *opening* operation with $\mathbf{S}(k)$. Fig. 1(a), (b), and (c) show a rabbit in the form of a 120×120 binary image, $\mathbf{M} \circ \mathbf{S}(12)$, and $\mathbf{M} - \mathbf{M} \circ \mathbf{S}(12)$, respectively. After the *opening* operation with $\mathbf{S}(k)$, the connected components in 4-neighborhoods are extracted from $\mathbf{M} \circ \mathbf{S}(k)$ and $\mathbf{M} - \mathbf{M} \circ \mathbf{S}(k)$. Then the set of binary images, $\mathcal{P}_{\mathbf{M}}(k) = \{\mathbf{M}_i(k) | i = 1, \dots, I_k\}$ is composed, where $\mathbf{M}_i(k)$, called a part, refers to a binary image and I_k is the number of binary images. In this context, the set of parts extracted from $\mathbf{M} \circ \mathbf{S}(k)$ and that extracted from $\mathbf{M} - \mathbf{M} \circ \mathbf{S}(k)$ are called the *body class* and *branch class*, respectively. Note that $\bigcup_{i=1}^{I_k} \mathbf{M}_i(k)$ is equal to \mathbf{M} , and any pair of binary images in $\mathcal{P}_{\mathbf{M}}(k)$ is disjoint. Fig. 1(d) shows $\mathcal{P}_{\mathbf{M}}(12)$ after extracting the connected components.

Apparently, there exist negligible parts in the *branch class*, enclosed by a circle in Fig. 1(d), which should be absorbed for the sake of compactness. In this paper, we adopt a simple measure, *i.e.* the notion of the part’s height with a certain threshold, to determine whether a part in the *branch class* is to be merged or not. Note that any proper measure, such as the area ratio between adjacent parts, can be used instead of our measure. Fig. 1(e) shows $\mathcal{P}_{\mathbf{M}}(12)$ after absorbing negligible parts. In this context, the boundary between the parts in Fig. 1(e) is not straight due to the *opening*

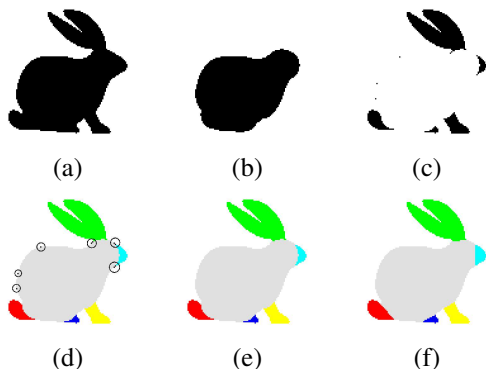


Fig. 1. The example of generating parts using the *opening* operation with $\mathbf{S}(12)$.

operation with the ball-shaped SE. Sometimes, this yields unexpectedly peculiar parts when the recursive decomposition stage described in Section 3 is performed. Therefore, we adopt an additional procedure to flatten the boundary between the parts, *i.e.* flattening procedure: When there exist two adjacent parts, $\mathbf{M}_{i_1}(k)$ in the *branch class* and $\mathbf{M}_{i_2}(k)$ in the *body class*, a *convex hull* can be generated for the elements of $\mathbf{M}_{i_1}(k)$ adjacent to those of $\mathbf{M}_{i_2}(k)$. Then the flattening procedure implies that $\mathbf{M}_{i_1}(k)$ absorbs the elements of $\mathbf{M}_{i_2}(k)$, which are included in the *convex hull*. Fig. 1(f) shows $\mathcal{P}_{\mathbf{M}}(12)$ after the flattening procedure.

2.2. Automatic selection using weighted convexity

Note that the generation of the parts for a given shape is performed for all possible k ’s, $k = 1, \dots, K$, where $K + 1$ is the radius of the ball-shaped SE when the *body class* becomes the empty set. In this context, $\mathcal{P}_{\mathbf{M}}(k)$, $k = 1, \dots, K$, are candidates for the output of the CMD. Now, it is necessary to define a measure for choosing the best candidate. In this paper, the *weighted convexity* for $\mathcal{P}_{\mathbf{M}}(k)$, $C_w(\mathcal{P}_{\mathbf{M}}(k))$, is introduced as a decision measure, given by

$$C_w(\mathcal{P}_{\mathbf{M}}(k)) = \sum_{i=1}^{I_k} \frac{N(\mathbf{M}_i(k))}{N(\mathbf{M})} C(\mathbf{M}_i(k)), \quad (2)$$

where $N(\cdot)$ and $C(\cdot)$ refer to the number of pixels representing 2-D shape and the convexity [3], respectively. Note that the *convexity* is in the interval $(0, 1]$. Then the output of the CMD for \mathbf{M} , $\mathcal{P}_{\mathbf{M}}$, is $\mathcal{P}_{\mathbf{M}}(k_{max})$, where

$$k_{max} = \arg \max_{k \in \{1, \dots, K\}} C_w(\mathcal{P}_{\mathbf{M}}(k)). \quad (3)$$

In other words, $\mathcal{P}_{\mathbf{M}}$ yields the maximum *weighted convexity* among the candidates. Finally, $\mathcal{P}_{\mathbf{M}} = \{\mathbf{M}_i | i = 1, \dots, I\}$ where \mathbf{M}_i refers to a part and I is the number of parts. Fig. 2 shows the excerpts of the candidates for $\mathcal{P}_{\mathbf{M}}$ of the rabbit. In this case, $\mathcal{P}_{\mathbf{M}}(12)$ of Fig. 2(c) becomes $\mathcal{P}_{\mathbf{M}}$ since it yields the maximum *weighted convexity*, 0.939.

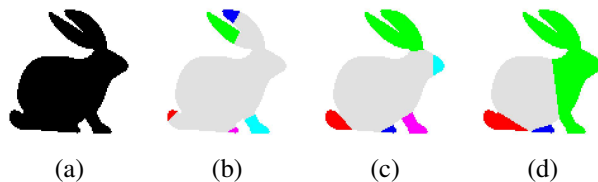


Fig. 2. The excerpts of the candidates for $\mathcal{P}_{\mathbf{M}}$ and its *weighted convexity*, $C_w(\mathcal{P}_{\mathbf{M}}(k))$: (a) $C_w(\mathbf{M}) = 0.750$, (b) $C_w(\mathcal{P}_{\mathbf{M}}(6)) = 0.836$, (c) $C_w(\mathcal{P}_{\mathbf{M}}(12)) = 0.939$, and (d) $C_w(\mathcal{P}_{\mathbf{M}}(26)) = 0.822$.

3. SHAPE DECOMPOSITION SCHEME

First, the proposed scheme performs once the CMD for a given shape, \mathbf{M} , which provides $\mathcal{P}_{\mathbf{M}}$. Although $\mathcal{P}_{\mathbf{M}}$ is usually adequate for an intuitive description, it generally requires some refinements, which depends on the complexity of the input shape. For example, Fig. 3(a) shows $\mathcal{P}_{\mathbf{M}}$ for the rabbit, and in this case it would be better if \mathbf{M}_3 , which contains two ears, were to be split. Therefore, in this paper, the CMD will be performed recursively in order to provide a more intuitive description. Actually, the recursive CMD would be terminated when no more parts can be split. However, if this were the case, it is likely that too many meaningless parts would be generated from the CMD in the *branch class* since this class generally represents minor details. Therefore, the *split criterion* is introduced, especially for the *branch class*, to determine whether a part in the *branch class* is to be split or not.

For the additional decomposition of a part in the *branch class* to be meaningful, it must be empirically observed that the CMD of that part yields at least two parts, each of which has only one adjacent part. Let us refer to this observation as the *split criterion*. When a part in the *branch class* satisfies the *split criterion*, it is split. In order to provide a more intuitive description, the recursive CMD with the *split criterion* will be performed until no more parts can be split. Let us refer to this as the recursive decomposition stage (RDS), and denote the output of the RDS for \mathbf{M} as $\hat{\mathcal{P}}_{\mathbf{M}} = \{\hat{\mathbf{M}}_i | i = 1, \dots, \hat{I}\}$ where $\hat{\mathbf{M}}_i$ refers to a part and \hat{I} is the number of parts. Fig. 3(a) shows $\mathcal{P}_{\mathbf{M}}$ for the rabbit, consisting of one part in the *body class*, \mathbf{M}_1 , and five parts in the *branch class*, \mathbf{M}_{2-6} . Fig. 3(b) is the result obtained after performing the CMD once for each part in Fig. 3(a), where \mathbf{M}_{1-3} and \mathbf{M}_5 are split, and \mathbf{M}_4 and \mathbf{M}_6 are not. Here, \mathbf{M}_1 belongs to the *body class*, and \mathbf{M}_3 is satisfied with *split criterion* but \mathbf{M}_2 and \mathbf{M}_5 are not. Therefore, as shown in Fig. 3(c), \mathbf{M}_1 and \mathbf{M}_3 are split, and \mathbf{M}_2 and \mathbf{M}_5 are not. In this way, the RDS proceeds until there is no part to be split. In the case of the rabbit, Fig. 3(c) refers to the final result of the RDS, $\hat{\mathcal{P}}_{\mathbf{M}}$.

From the point of view of compactness, it can be observed that there are over-decomposed parts, enclosed by a circle in Fig. 3(c) since the RDS performs the recursive CMD in a greedy manner. Therefore, a final merging pro-

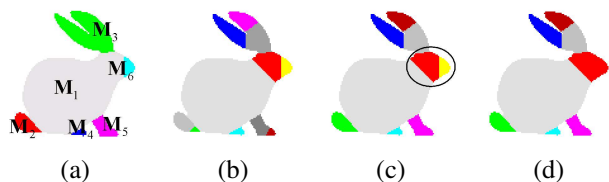


Fig. 3. An example of the RDS and the IMS for the rabbit.

cedure is required after the RDS. In this paper, the weighted convexity difference (WCD) and the *merging criterion* are introduced as decision measures for the merging procedure and for evaluating the suitability of the merging parts, respectively. In this context, the WCD refers to the difference of the *weighted convexity* during the merging of the parts.

Assume that $\hat{\mathcal{P}}_{\mathbf{M}}$, the output of the RDS for \mathbf{M} , has \hat{I} parts ($\hat{\mathbf{M}}_i, i = 1, \dots, \hat{I}$). Then the WCD is defined for two adjacent parts, $\hat{\mathbf{M}}_{i_1}$ and $\hat{\mathbf{M}}_{i_2}$ in $\hat{\mathcal{P}}_{\mathbf{M}}$, as follows:

$$D(\hat{\mathbf{M}}_{i_1}, \hat{\mathbf{M}}_{i_2}) = C_w(\{\hat{\mathbf{M}}_{i_1}, \hat{\mathbf{M}}_{i_2}\}) - C(\hat{\mathbf{M}}_{i_1} \cup \hat{\mathbf{M}}_{i_2}). \quad (4)$$

Note that the WCD is the difference between the *weighted convexity* of the two parts, $\hat{\mathbf{M}}_{i_1}$ and $\hat{\mathbf{M}}_{i_2}$, and that of the merged part, $\hat{\mathbf{M}}_{i_1} \cup \hat{\mathbf{M}}_{i_2}$. Then the *merging criterion* associated with the WCD is

$$D(\hat{\mathbf{M}}_{i_1}, \hat{\mathbf{M}}_{i_2}) \leq \min\left(t_L, \frac{t_G}{f}\right), \quad (5)$$

where $f = \frac{N(\hat{\mathbf{M}}_{i_1}) + N(\hat{\mathbf{M}}_{i_2})}{N(\mathbf{M})}$, and t_L and t_G refer to thresholds for the WCD and the WCD multiplied by f , respectively. Especially, t_G implies the allowable convexity reduction when the two adjacent parts are merged by considering the *weighted convexity* of all parts in a given shape. Finally, the merging procedure is performed iteratively until no more adjacent parts are satisfied with (5). In this context, it is applied to two adjacent parts, $\hat{\mathbf{M}}_{i_1}$ and $\hat{\mathbf{M}}_{i_2}$, of which $fD(\hat{\mathbf{M}}_{i_1}, \hat{\mathbf{M}}_{i_2})$ is the minimum value of this function for all adjacent parts. Let us refer to it as the iterative merging stage (IMS), and denote the output of the IMS for \mathbf{M} as $\tilde{\mathcal{P}}_{\mathbf{M}} = \{\tilde{\mathbf{M}}_i | i = 1, \dots, \tilde{I}\}$ where $\tilde{\mathbf{M}}_i$ refers to a part and \tilde{I} is the number of parts. Note that the IMS controls the trade-off, *i.e.* whether $\tilde{\mathcal{P}}_{\mathbf{M}}$ is to be the compact representation or that required to obtain the maximum *weighted convexity*. Fig. 3(d) shows the results of the IMS, $\tilde{\mathcal{P}}_{\mathbf{M}}$, with $t_L = 0.03$ and $t_G = 0.005$ for the rabbit, where t_L and t_G are determined experimentally. More specifically, the nine parts in Fig. 3(c), where $C_w(\hat{\mathcal{P}}_{\mathbf{M}}) = 0.971$, become eight parts in Fig. 3(d), where $C_w(\tilde{\mathcal{P}}_{\mathbf{M}}) = 0.970$, with a reduction of the *weighted convexity* by 0.001.

4. EXPERIMENTAL RESULTS

In this section, we present experimental results for various and modified 2-D shapes in order to examine the qualitative performance of the proposed scheme. Although the CMD is performed recursively, the proposed scheme can yield the decomposition result in a few iterations by virtue of the *split criterion*. In addition, it is worthy to note that the proposed scheme worked well in all of the experiments although the thresholds for the *merging criterion* were always set to $t_G = 0.005$ and $t_L = 0.03$.

To perform the subjective evaluation of the proposed scheme, we applied the proposed scheme to the 2-D shapes

given in [1] and [2]. Fig. 4 shows the decomposition results for four 2-D shapes, provided in the form of 40×40 binary images. Note that the proposed scheme yielded reasonable decomposition results similar to those of [1]. Especially, the number of parts is significantly reduced by virtue of the IMS using the *merging criterion* compared with [1]. On the other hand, Fig. 4(b) has two redundant parts in the upper region of the truck. Actually, the ability of the proposed scheme to extract the exact polygon-shaped part is somewhat unsatisfactory due to the characteristics of the ball-shaped SE. Fig. 5 shows the decomposition results for four 2-D shapes, provided in the form of 120×120 binary images. Note that the decomposition results are observed to be in good agreement with the perceived parts as shown in [2]. Especially, the proposed scheme is able to extract the tail part for Fig. 5(c) and (d) in contrast to [2]. On the other hand, Fig. 5(a) is somewhat over-decomposed since the proposed scheme does not consider the concavities in the boundary of a given shape.

To demonstrate its robustness, we applied the proposed scheme to the modified rabbits and hands. Fig. 6 shows the decomposition results for the scaled, rotated, and noise-corrupted 2-D shapes of the rabbit. In this experiment, the noise for the 2-D shape, as shown in Fig. 6(d), was generated as described in [1]. All of the perturbed shapes in Fig. 6 yielded the same decomposition results as shown in Fig. 3(d). Fig. 7 shows the decomposition results for the deformed and occluded 2-D shapes given in [5]. Note that all of the shapes in Fig. 7 yielded the same or reasonable decomposition results. From Figs. 6 and 7, it is believed that the proposed scheme is quite robust not only to scaling, rotation, and noise, but also to shape deformation and occlusion.

5. CONCLUSION

In this paper, a new decomposition scheme for 2-D shape was presented. To begin with, the constrained morphological decomposition (CMD) method, based on the *opening* operation and the *weighted convexity*, was proposed. The proposed scheme performs the CMD procedure once for a given shape, then recursively for each part using the *split criterion*. Finally, the use of the *merging criterion* was adopted by considering the change of the *weighted convexity* in the form of the weighted convexity difference (WCD). From the experimental results, it was found that the proposed scheme yields an intuitive description, and provides robustness to scaling, rotation, noise, shape deformation, and occlusion. Therefore, the proposed scheme can be expected to generate perceptual graph-based representations for shape-related applications such as those involving content-based retrieval and object recognition.

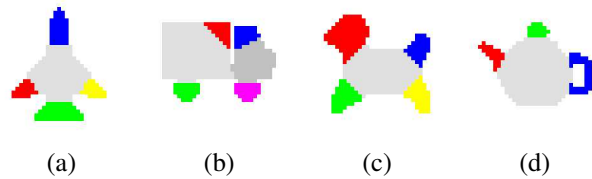


Fig. 4. Experimental results for the four 2-D shapes in [1].

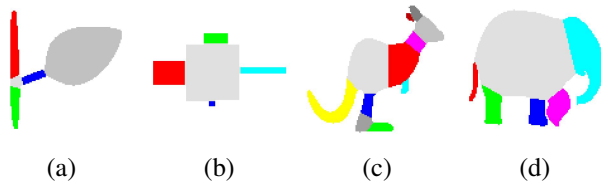


Fig. 5. Experimental results for the four 2-D shapes in [2].

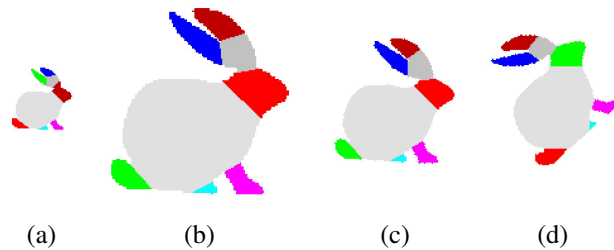


Fig. 6. Experimental results for the modified rabbits: (a) the 0.5 scaled shape, (b) the 1.5 scaled shape, (c) the 45 degrees rotated shape, and (d) the 10% noise-corrupted shape.

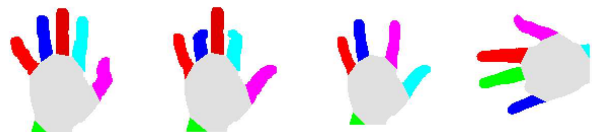


Fig. 7. Experimental results for the modified hands in [5].

6. REFERENCES

- [1] J. Xu, "Morphological decomposition of 2-d binary shapes into convex polygons: a heuristic algorithm," *IEEE Trans. IP*, vol. 10, no. 1, pp. 61–71, January 2001.
- [2] K. Siddiqi and B. B. Kimia, "Parts of visual form: computational aspects," *IEEE Trans. PAMI*, vol. 17, no. 3, pp. 239–251, March 1995.
- [3] P. L. Rosin, "Shape partitioning by convexity," *IEEE Trans. SMC-A*, vol. 30, no. 2, pp. 202–210, March 2000.
- [4] A. P. Pentland, "Recognition by parts," *Proc. ICCV*, pp. 612–620, June 1987.
- [5] T. B. Sebastian, P. N. Klein, and B. B. Kimia, "Recognition of shapes by editing shock graphs," *Proc. ICCV*, vol. 1, pp. 755–762, July 2001.